

Screened Raman response in two-dimensional $d_{x^2-y^2}$ -wave superconductors: Relative intensities in different symmetry channels

Fabian Wenger

NEC Research Institute, 4 Independence Way, Princeton, New Jersey 08540*
and Institute of Theoretical Physics, Chalmers University of Technology, 412 96 Göteborg, Sweden

Mikael Käll

Department of Solid State Physics, Risø National Laboratory, 4000 Roskilde, Denmark
and Department of Physics, Chalmers University of Technology, 412 96 Göteborg, Sweden*

(Received 27 June 1996)

We analyze the Raman-scattering response in a two-dimensional $d_{x^2-y^2}$ -wave superconductor and point out a strong suppression of relative intensity in the screened A_{1g} channel compared to the B_{1g} channel for a generic tight-binding model. This is in contrast with the observed behavior in high- T_c superconductors. [S0163-1829(97)01701-3]

In recent years, a number of experiments have supported the view that high- T_c superconductors might have a gap function of $d_{x^2-y^2}$ -wave symmetry, for a recent review see, e.g., Ref. 1. There have been contradictory claims^{2,3} whether the observed symmetry-dependent electronic Raman scattering⁵ is consistent with $d_{x^2-y^2}$ -wave symmetry. It has been established by Devereaux *et al.* that the qualitative behavior of the *screened* Raman response qualitatively reproduces the observed symmetry dependence in the cuprate superconductors, a crucial point being the presence of a peak in B_{1g} symmetry associated theoretically with $2\Delta_{\max}$ which is absent in the A_{1g} channel due to screening. The original calculations were performed by expanding the Raman vertices in Fermi-surface harmonics and retaining the lowest non-vanishing terms in each symmetry channel. The relative intensities of these couplings remained undetermined and likewise the relative intensities of the symmetry-dependent Raman response. To gain insight into the quantitative aspects, it is therefore important to analyze the situation for a generic tight-binding band structure with given parameters. This quantitative analysis is the main purpose of our study and we find a discrepancy in the relative intensity of the screened A_{1g} channel which is only a small fraction of the B_{1g} response of the same band.

According to the results of Abrikosov, Fal'kovskii, and Genkin⁶ the imaginary part of the unscreened nonresonant Raman response in a superconductor at $T=0$ is proportional to

$$\chi''_0(q=0, \omega) = \int \frac{d^2k}{(2\pi)^2} \delta(\omega - 2E(k)) \frac{|\Delta(k)|^2}{E(k)^2} |\gamma(k)|^2, \quad (1)$$

if we neglect the wave vector q of the incoming photons compared to the extension of the Brillouin zone and if the penetration depth is much larger than the coherence length. We denote the gap function by $\Delta(k)$, the single-particle energy by $\xi(k)$ and the quasiparticle energy by $E(k) = \sqrt{\xi(k)^2 + |\Delta(k)|^2}$. $\gamma(k) = \vec{e}_i [\partial^2 \xi(k) / (\partial k_m \partial k_n)] \vec{e}_f$ denotes the nonresonant Raman vertex with initial and final

unit polarization vectors $\vec{e}_{i,f}$. To simplify the discussion we set $e = \hbar = m = a = 1$ (a is the lattice constant), hence χ'' is measured in units of energy. We assume here a quasi-two-dimensional (2D) situation such that the integration in the third momentum direction can be neglected.

The screened Raman response in the same limit has been calculated by Klein and Dierker⁷ and is given by

$$\chi'' = \chi''[\gamma, \gamma] - \left(\frac{\chi[\gamma, 1] \chi[1, \gamma]}{\chi[1, 1]} \right)'', \quad (2)$$

where we define

$$\chi''[a, b] = \int \frac{d^2k}{(2\pi)^2} \delta(\omega - 2E(k)) \frac{|\Delta(k)|^2}{E(k)^2} a(k) b(k)^*. \quad (3)$$

The first term in Eq. (2) is just the unscreened response and the real part χ' which is needed for the second part is obtained by a Kramers-Kronig transformation of the imaginary part χ'' . If we split $\gamma(k)$ into a sum of contributions which transform according to the different representation of the symmetry group of the lattice, the second term vanishes for all nontrivial representations, since the remaining terms of the integrand are supposed to transform trivially under any lattice symmetry.

In the following the single-particle energy $\xi(k)$ will be described by a single tight-binding band with square D_4 symmetry:

$$\xi(k) = -\mu - 2t(\cos k_x + \cos k_y) - 4t' \cos k_x \cos k_y, \quad (4)$$

where t and t' are the nearest- and next-nearest-neighbor hopping and μ is the chemical potential to adjust the filling factor. We use a $d_{x^2-y^2}$ -wave gap function

$$\Delta(k) = \frac{\Delta}{2} (\cos k_x - \cos k_y). \quad (5)$$

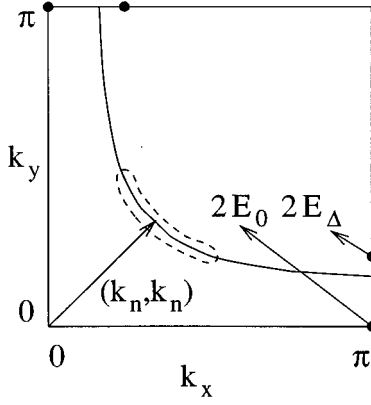


FIG. 1. A schematic drawing of a $\text{YBa}_2\text{Cu}_3\text{O}_{7-\delta}$ -like Fermi surface (full line) in the first quadrant of the Brillouin zone. Dashed curves illustrate constant $E(k) \ll \Delta$. Fat dots mark the location of van Hove singularities which give rise to peaks in the Raman response at $2E_\Delta$ and $2E_0$. The location of the node is indicated by the vector (k_n, k_n) .

The Raman vertex for given initial and final polarization angles (measured from the x axis which is defined to be along the Cu-O bond direction) is given by

$$\begin{aligned} \gamma(k) &= \cos(\alpha - \beta)[t(\cos k_x + \cos k_y) + 4t' \cos k_x \cos k_y] \\ &\quad + \cos(\alpha + \beta)t(\cos k_x - \cos k_y) \\ &\quad - \sin(\alpha + \beta)4t' \sin k_x \sin k_y, \\ &= \cos(\alpha - \beta)\gamma_{A_{1g}}(k) + \cos(\alpha + \beta)\gamma_{B_{1g}}(k) \\ &\quad + \sin(\alpha + \beta)\gamma_{B_{2g}}(k). \end{aligned} \quad (6)$$

The first term has A_{1g} symmetry, the second B_{1g} , and the third B_{2g} . Note that $\alpha = \beta = \pi/4$ [corresponding to scattering configuration $z(x+y, x+y)\bar{z}$ in Porto's notation] measures $\gamma_{A_{1g}}(k) + \gamma_{B_{2g}}(k)$. As has been pointed out before,² the A_{1g} contribution is mixed with at least one other channel for all angles. Pure B_{1g} symmetry can be achieved by choosing $\alpha = \pi/4$ and $\beta = -\pi/4$. Pure B_{2g} symmetry can be achieved by choosing $\alpha = 0$ and $\beta = \pi/2$.

For a qualitative analysis we note that if the factor $|\Delta(k)|^2/E(k)^2 |\gamma(k)|^2$ would be absent in Eq. (1) the unscreened Raman response would be proportional to the quasiparticle density of states $n(\omega/2)$. This quantity was analyzed in Ref. 8 and the characteristic features of $n(\omega)$ are in case $|2t'/t| < 1$ and $\Delta \ll t$: (i) an approximately linear density of states at energies below $\Delta = \Delta_{\max}$ and (ii) two logarithmic van Hove singularities at energies E_Δ and E_0 . We have $E_\Delta \approx \Delta$ and $E_0 = \sqrt{(4t' - \mu)^2 + |\Delta|^2}$, E_0 is related to the tight-binding band van Hove singularity at the zone boundary (see Fig. 1). Since the other terms in the integrand (1) are regular [analyticity of the tight-binding band; $0 \leq |\Delta(k)|^2/E(k)^2 \leq 1$ and zero only at nodes], these van Hove singularities are in general present in the Raman response at $2E_\Delta$ and $2E_0$ unless $\gamma(k)$ is zero for symmetry reasons or removed by screening in the A_{1g} symmetry.

In the $\text{YBa}_2\text{Cu}_3\text{O}_{7-\delta}$ -like Fermi surface, displayed in Fig. 1, the $2E_\Delta$ van Hove singularity lies away from the

main axes and could, in principle, be present in the B_{2g} channel but since $\gamma_{B_{2g}}(k)$ vanishes on the whole zone boundary, no van Hove singularity appears in B_{2g} at $2E_\Delta$. The "normal" van Hove singularity at $2E_0$ on the other hand vanishes by symmetry in the B_{2g} channel.

Before we analyze the two cases numerically we derive the asymptotic behavior of $\chi''(\omega)$. As Raman vertices we use: $\gamma_{A_{1g}}$, $\gamma_{B_{1g}}$, and $\gamma_{B_{2g}}$ neglecting the dependence on α and β . In an actual measurement one should, of course, weight those contributions with the appropriate prefactors (note that contributions from mixed symmetries, e.g., $\propto \gamma_{B_{1g}}\gamma_{B_{2g}}$ vanish of course). Following the analysis of Ref. 8 we can make a variable change from (k_x, k_y) to $(u = \xi_k, v = \Delta_k)$. The Jacobian J and the Raman vertex can be expanded in a Taylor series around the node, i.e., $u = v = 0$. The leading terms are

$$J(u, v) = J_0 + J_1 u + J_2 u^2 + J_3 v^2 + \dots, \quad (8)$$

$$\gamma_{A_{1g}} = \gamma_0 + \gamma_1 u + \gamma_2 u^2 + \gamma_3 v^2 + \dots, \quad (9)$$

$$\gamma_{B_{1g}} = 2t/\Delta v, \quad (10)$$

$$\gamma_{B_{2g}} = 4t' \sin^2 k_n + \dots, \quad (11)$$

where we have made use of the symmetry properties of J and $\gamma_{A_{1g}}$ which cannot contain odd powers of v . k_n is given by the location of the four nodes at $(\pm k_n, \pm k_n)$ and $(\mp k_n, \pm k_n)$. Since B_{1g} and B_{2g} are not affected by screening we immediately arrive at

$$\chi''(\omega) \approx \frac{J_0}{4\pi} \times \begin{cases} (3t^2/4\Delta^2)\omega^3; B_{1g} \\ 16t'^2 \sin^2 k_n \omega; B_{2g} \end{cases} \quad (12)$$

for $\omega \ll 2E_\Delta$; $J_0 = 1/[2\Delta(t + 2t' \cos k_n) \sin^2 k_n]$. If we use these asymptotic forms at $\omega \approx \Delta$ the B_{1g} response is enhanced by a factor $(t/t')^2$ over the B_{2g} channel. Since $\gamma_{A_{1g}} = -\mu/2 + 2t' \cos^2 k_n - u/2 + \dots$ the unscreened response for A_{1g} is

$$\chi_0''(\omega) \approx \frac{J_0}{4\pi} (-\mu/2 + 2t' \cos^2 k_n)^2 \omega; A_{1g} \text{ unscreened.} \quad (13)$$

Therefore the unscreened response at low frequencies is linear as in B_{2g} and for $k_n \approx \pi/2$ we have

$$\chi_{B_{2g}}''(\omega)/\chi_{0, A_{1g}}''(\omega) \xrightarrow{\omega \rightarrow 0} 64 \frac{t'^2}{\mu^2}. \quad (14)$$

The low-frequency asymptotics of the screened A_{1g} response is not as simple and is more conveniently determined numerically.

For comparison with $\text{YBa}_2\text{Cu}_3\text{O}_{7-\delta}$ we take from Ref. 9 the values $t = 250$ meV, $t' = -112.5$ meV, a hole doping of 25% fixes $\mu = -365$ meV and we choose $\Delta = 20$ meV. The results for the Raman response are displayed in Fig. 2 (fat lines). Small changes of t, t', μ, Δ lead only to minor quantitative changes. To illustrate this we have plotted in Fig. 2 (fine lines) the Raman response with a smaller value of $\mu = -420$ meV which enhances the weight of the van Hove singularities and shifts them closer together. The $2E_\Delta$ peak is

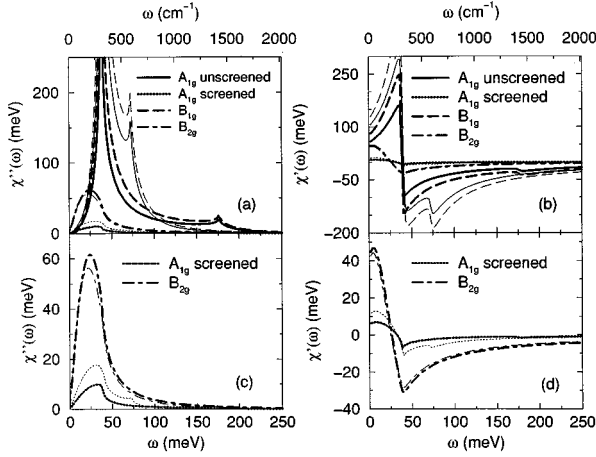


FIG. 2. (a) $\chi''(\omega)$ for different symmetries modeling $\text{YBa}_2\text{Cu}_3\text{O}_{7-\delta}$ with $t=250$ meV, $t'=-112.5$ meV, $\Delta=20$ meV. Fat lines are for $\mu=-365$ meV, fine lines for $\mu=-420$ meV. (b) $\chi'(\omega)$ for identical parameters as in (a). (c) Enlarged portion of (a) containing $\chi''(\omega)$ for screened A_{1g} and B_{2g} . (d) Enlarged portion of (b) containing $\chi'(\omega)$ for screened A_{1g} and B_{2g} .

enhanced since it lies near the saddle point of the normal band and the $2E_0$ peak becomes more visible since it is now at a lower excitation energy, i.e., $|\Delta(k)|^2/E(k)^2$ is considerably larger. Apart from these shifts and overall increase of the intensity the spectrum looks rather similar. For the sake of completeness we also plot in Fig. 2 the real part of the Raman response function which can be associated with the frequency shift of the optical Raman-active phonon modes within a random-phase approximation.² The important features of the numerical results are in qualitative agreement with earlier studies.² They are concerning the imaginary part χ'' of the response function: the B_{1g} response is the only symmetry which exhibits a peak at 2Δ , the screening removes the corresponding peak in A_{1g} symmetry, and only leaves a broad shoulder as in the B_{2g} case which has its maximum clearly below 2Δ . The crucial observation is however that screening is also extremely effective in *reducing the relative intensity of the A_{1g} contribution*, such that it would almost not show up in mixture with other channels. There are three main sources of error for these numerical results: (i) the discrete lattice of momentum states, (ii) the accuracy of the Kramers-Kronig transform and (iii) extinction when calculating the screened values close to a van Hove singularity in the density of states. (i) would wash out sharp features of χ'' , and (iii) would show up in erratic changes of the screened A_{1g} response at peak values of the unscreened response. None of those signs is observed in Figs. 2. The accuracy of the Kramers-Kronig transform is demonstrated by the absence of these signs even in the real parts χ' . We are therefore confident that the numerical values in the screened A_{1g} channel are indeed significant.

The comparison with the experimental data assumes that the orthorhombic deformations in $\text{YBa}_2\text{Cu}_3\text{O}_{7-\delta}$ are of minor influence for the superconductivity in the CuO_2 planes which is supposed to be modeled by our choice of $\xi(k)$ and $\Delta(k)$. Other possible superconducting structures apart from the CuO_2 planes, e.g., the CuO chains in $\text{YBa}_2\text{Cu}_3\text{O}_{7-\delta}$,

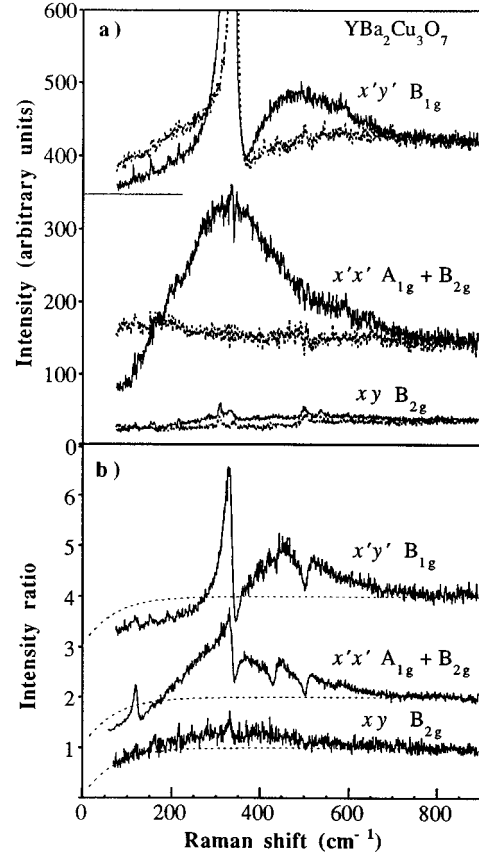


FIG. 3. (a) a - b plane polarized Raman response of a fully oxygenated $\text{YBa}_2\text{Cu}_3\text{O}_{7-\delta}$ crystal, recorded just above (95 K, full line) and well below (10 K, dotted line) the transition temperature $T_c = 91$ K. Data for the scattering configurations $x'y'$, xy , and $x'x'$ are shown with subtraction of phonon contribution (no subtraction has been performed for the 340 cm^{-1} phonon in the $x'y'$ symmetry). The $x'y'$ spectrum has been shifted by 350 intensity units as indicated for clarity. (b) The Raman spectrum ratio of the intensities in the superconducting/normal state (raw data) is plotted together with the ratio of the corresponding Bose factors (dashed line).

might complicate the analysis. Figure 3 shows a - b plane polarized Raman spectra of a $\text{YBa}_2\text{Cu}_3\text{O}_{6.97}$ single crystal ($T_c=91$ K, $\delta T_c = 0.2$ K) recorded just above (95 K) and well below (10 K) the superconducting transition. Data for the scattering configurations $x'y'$, xy , and $x'x'$ are shown with and without phonon subtraction (except the 340 cm^{-1} B_{1g} mode) together with the ratio between the 10 and 95 K raw data and the corresponding Bose factor ratio (dashed line). For clarity the curves have been shifted vertically, but we indicate the corresponding intensity in arbitrary but fixed units on the y axis. The measurements were performed in a near-backscattering geometry with 4 mW of incident radiation ($\lambda = 5145$ Å) focused to a 50 μm diameter spot, using a standard Raman setup (SPEX 1877 with CCD detection, resolution 4 cm^{-1}). The sample was mounted on the cold finger of a liquid-He cryostat. In the tetragonal approximation $x'y'$, xy , and $x'x'$ correspond to $(\alpha, \beta) = (\pi/4, -\pi/4), (0, \pi/2)$, and $(\pi/4, \pi/4)$, which according to Eq. (7) select $\gamma_{B_{1g}}(k)$, $\gamma_{B_{2g}}(k)$, and $\gamma_{A_{1g}}(k) + \gamma_{B_{2g}}(k)$, respectively. In the $x'y'$ and $x'x'$ spectra of Fig. 3 a strong

redistribution of the continuum scattering intensity below T_c is evident; i.e., the intensity at low frequencies decreases more than expected from the Bose population factor and a peak develops at higher frequencies. The continuum peak occur at $\approx 330 \text{ cm}^{-1} \approx 40 \text{ meV}$ for the $x'x'$ geometry and at $\approx 470 \text{ cm}^{-1} \approx 60 \text{ meV}$ for the $x'y'$ geometry. The continuum redistribution is accompanied by the well-known phonon renormalization (i.e., change in phonon frequencies, linewidths, and intensities) and both effects show up clearly in the ratio between Raman spectra recorded in superconducting and normal state which is plotted together with the ratio of the corresponding Bose factors. The scattering in xy geometry increases at higher frequency below T_c , forming a broad peak somewhat similar to the $x'x'$ case, but there is no sign for a compensating intensity decrease at low frequencies and thus no real intensity redistribution. In order to obtain the detailed shape of the continuum response function above and below T_c , it may be advantageous to subtract the sharp phonon features. In the $x'x'$ spectra this is a fairly straightforward, although tedious, procedure but the resulting smooth spectra does not show any new features that are not obvious also in the spectral ratio. In the $x'y'$ case the 340 cm^{-1} oxygen phonon is not subtracted (a possible subtraction scheme has been described by Devereaux *et al.*⁴). We can nevertheless clearly identify the relative size and position of the continuum peak at $\approx 470 \text{ cm}^{-1}$ for the $x'y'$ geometry.

The present data, as well as earlier studies on both $\text{YBa}_2\text{Cu}_3\text{O}_{7-\delta}$ (Refs. 5,2 and 3) and $\text{Bi}_2\text{Sr}_2\text{CaCu}_2\text{O}_{8+\delta}$ (Refs. 10 and 11) show that the B_{1g} response is clearly more intense and peaks at a higher energy than the B_{2g} response in the superconducting state. This is in qualitative and quanti-

tative agreement with the theoretical results. The point we want to focus on here however is that for $(\alpha, \beta) = (\pi/4, \pi/4)$, i.e., $x'x'$, the electronic scattering is clearly more intense than for pure B_{2g} , i.e., xy , indicating a large A_{1g} component, in *quantitative* contradiction with the theoretical results for the screened A_{1g} response. To invoke that the screening is not effective does not help due to the absence of a continuum peak in $x'x'$ where the continuum peak in $x'y'$ is located. Thus we find it difficult to reconcile the theoretical Raman response for a 2D $d_{x^2-y^2}$ -wave superconductor with a generic tight-binding band with the experimentally observed relative intensities for cuprate superconductors. Better agreement may require a more realistic band structure including all bands within an energy comparable to the incoming (outgoing) photon energy measured from the Fermi energy and also correlation effects which cannot be included in a simple tight-binding spectrum. If the resulting Raman vertex $\gamma(k)$ would have a strongly dominating bare A_{1g} component compared to the B_{1g} part, the screened A_{1g} Raman response could be of the same order of magnitude as the B_{1g} response. This possibility remains to be investigated further.

In summary we found that the electronic Raman scattering of a 2D $d_{x^2-y^2}$ -wave superconductor in the screened A_{1g} channel is only a tiny fraction of the B_{1g} response which is not in agreement with the observed spectra of cuprate superconductors.

F.W. would like to thank the Superconductivity Consortium at Chalmers and the Schweizerischer Nationalfonds for financial support.

*Present address.

¹D.J. Scalapino, Phys. Rep. **250**, 329 (1995).

²T.P. Devereaux *et al.*, Phys. Rev. Lett. **72**, 396 (1994); T.P. Devereaux *et al.*, *ibid.* **72**, 3291 (1994); T.P. Devereaux, Phys. Rev. B **50**, 10 287 (1994); T.P. Devereaux and D. Einzel, *ibid.* **51**, 16 336 (1995).

³M.C. Krantz and M. Cardona, Phys. Rev. Lett. **72**, 3290 (1994); J. Low Temp. Phys. **99**, 205 (1995).

⁴T.P. Devereaux, A. Virosztek, and A. Zawadowski, Phys. Rev. B **51**, 505 (1995).

⁵S.L. Cooper *et al.*, Phys. Rev. B **37**, 5920 (1988); R. Hackl *et al.*, *ibid.* **38**, 7133 (1988).

⁶A.A. Abrikosov and L.A. Fal'kovskii, Sov. Phys. JETP **13**, 179 (1961) [Zh. Eksp. Teor. Fiz. **40**, 262 (1961)]; A.A. Abrikosov and V.M. Genkin, Sov. Phys. JETP **38**, 417 (1974) [Zh. Eksp. Teor. Fiz. **65**, 842 (1973)].

⁷M.V. Klein and S.B. Dierker, Phys. Rev. B **29**, 4976 (1984).

⁸F. Wenger and S. Östlund, Phys. Rev. B **47**, 5977 (1993).

⁹P. Monthoux and D. Pines, Phys. Rev. B **47**, 6069 (1993).

¹⁰D. Kirillov *et al.*, Phys. Rev. B **38**, 11 955 (1988).

¹¹C. Kendziora and A. Rosenberg, Phys. Rev. B **52**, R9867 (1995).